

Spatial and temporal effects of drought on soil CO₂ efflux in a cacao agroforestry system in Sulawesi, Indonesia

O. van Straaten¹, E. Veldkamp¹, M. Köhler², and I. Anas³

¹Buesgen-Institute, Soil Science of Tropical and Subtropical Ecosystems, Georg-August-University of Goettingen, Buesgenweg 2, 37075 Goettingen, Germany

²Burckhardt-Institute, Tropical Silviculture and Forest Ecology, Georg-August-University of Goettingen, Buesgenweg 2, 37075 Goettingen, Germany

³Department of Soil Science, Faculty of Agriculture, Bogor Agricultural University (IPB), Jl. Raya Pajajaran Bogor 16143, Indonesia

Received: 25 November 2009 – Published in Biogeosciences Discuss.: 15 December 2009

Revised: 4 April 2010 – Accepted: 7 April 2010 – Published: 9 April 2010

Abstract. Climate change induced droughts pose a serious threat to ecosystems across the tropics and sub-tropics, particularly to those areas not adapted to natural dry periods. In order to study the vulnerability of cacao (*Theobroma cacao*) – *Gliricidia sepium* agroforestry plantations to droughts a large scale throughfall displacement roof was built in Central Sulawesi, Indonesia. In this 19-month experiment, we compared soil surface CO₂ efflux (soil respiration) from three roof plots with three adjacent control plots. Soil respiration rates peaked at intermediate soil moisture conditions and decreased under increasingly dry conditions (drought induced), or increasingly wet conditions (as evidenced in control plots). The roof plots exhibited a slight decrease in soil respiration compared to the control plots (average 13% decrease). The strength of the drought effect was spatially variable – while some measurement chamber sites reacted strongly (responsive) to the decrease in soil water content (up to $R^2 = 0.70$) ($n = 11$), others did not react at all (non-responsive) ($n = 7$). A significant correlation was measured between responsive soil respiration chamber sites and sap flux density ratios of cacao ($R = 0.61$) and *Gliricidia* ($R = 0.65$). Leaf litter CO₂ respiration decreased as conditions became drier. The litter layer contributed approximately 3–4% of the total CO₂ efflux during dry periods and up to 40% during wet periods. Within days of roof opening soil CO₂ efflux rose to control plot levels. Thereafter, CO₂

efflux remained comparable between roof and control plots. The cumulative effect on soil CO₂ emissions over the duration of the experiment was not significantly different: the control plots respired $11.1 \pm 0.5 \text{ Mg C ha}^{-1} \text{ yr}^{-1}$, while roof plots respired $10.5 \pm 0.5 \text{ Mg C ha}^{-1} \text{ yr}^{-1}$. The relatively mild decrease measured in soil CO₂ efflux indicates that this agroforestry ecosystem is capable of mitigating droughts with only minor stress symptoms.

1 Introduction

In recent decades, Indonesia has experienced severe droughts which were related to El Niño Southern Oscillation (ENSO) events (Quinn et al., 1978; Sheffield and Wood, 2008). Some climate prediction models suggest that droughts in Indonesia may become more frequent and more severe in the future (Sheffield and Wood, 2008; Timmermann et al., 1999). Changes in precipitation patterns due to climatic change, including droughts, will have direct effects on agricultural productivity (Sivakumar et al., 2005) and the terrestrial biosphere carbon cycle (Tian et al., 2000). Understanding how ecosystems and specifically carbon dynamics respond to droughts is important given the feedback potentials to the atmosphere from carbon dioxide (CO₂) emissions. Decreases in precipitation have been shown to affect plant root dynamics, litter fall, soil organic matter decomposition, nutrient mineralization rates, as well as soil aeration - which in turn affects gas diffusion and microbial processes (Davidson et al., 2004). Exactly how an ecosystem will react to drought is



Correspondence to: O. van Straaten
(ostraat@gwdg.de)

largely dependent on the mechanisms it has available to adapt to droughts. The presence or absence of deep root systems is one such response mechanism. Studies carried out in tropical forests of Latin America suggest that ecosystems with deep rooted trees are more capable of mitigating drought effects (Davidson et al., 2004; Nepstad et al., 1994).

Droughts in Indonesia pose a potential threat to both natural forest ecosystems and agricultural production systems for example cacao (*Theobroma cacao* L.). In the last 25 years, Indonesia has experienced a boom in cocoa production and has since become the third largest producer of cocoa beans worldwide (FAO, 2009). Nearly 80% of the cocoa beans produced in Indonesia are grown in Sulawesi. It is unknown how well cacao agroforestry plantations adapt to drought conditions, although a recent socio-economic survey by Keil et al. (2008) in central Sulawesi found that cocoa production is vulnerable to drought. Unlike cacao trees which tend to have a shallow rooting architecture (Kummerow et al., 1982), agroforestry over-story trees such as *Gliricidia* (*Gliricidia sepium* (Jacq.) Kunt ex Steud.) often have deeper root systems.

To date, little has been published on below-ground carbon dynamics in agroforestry systems (Bailey et al., 2009; Hergoualc'h et al., 2008; Oelbermann et al., 2006), and as far as we are aware, no soil CO₂ efflux measurements have been carried out in tropical agroforestry systems in relation to drought stress.

In this experiment, we investigated how soil CO₂ efflux in a cacao – *Gliricidia* agroforestry plantation in central Sulawesi, Indonesia reacted to an experimental drought. In an earlier paper by Schwendenmann et al. (2010) it was shown that this agroforest was surprisingly resilient to drought which was explained by a combination of complementary use of soil water resources and acclimation. The specific research objectives for this study were twofold:

1. to determine how belowground CO₂ production and surface soil CO₂ efflux reacted to a simulated drought and the subsequent rewetting phase;
2. to identify the controls driving CO₂ production.

At the beginning of the experiment we suspected that this agroforestry system would be vulnerable to drought stress and hypothesized that soil respiration rates would show strong decreases across the plantation. After the end of the simulated drought we expected a CO₂ production flush in the drought plots.

2 Materials and methods

2.1 Site description

The drought simulation experiment was conducted in a seven year old cacao agroforestry plantation on the western periphery of the Lore Lindu National Park (1.552° S, 120.020° E)

in Central Sulawesi, Indonesia at an elevation of 560 m above sea level (asl). Established in December 2000, the plantation was composed of a *Gliricidia* overstory (~330 trees ha⁻¹) and a cacao understory (~1030 trees ha⁻¹). The ground was largely devoid of undergrowth herbs and grasses except for a few patches of grass in open areas. We selected a site that was located on a gentle slope (8–12°), where the ground water table (>4.5 m) was deeper than the tree rooting zone. The region experiences two mild rainy seasons per year. The average annual precipitation from 2002 to 2006 at the Gimpu meteorological station (417 m a.s.l.) five kilometers south of the experimental site was 2092 mm. The mean annual temperature was 25.5 °C (Schwendenmann et al., 2010).

The soil has been classified as a Cambisol with a sandy loam texture (Leitner and Michalzik, unpublished data). The top 75 cm of soil has a relatively homogeneous texture, a stone content of 15–25% and a bulk density of 1.31±0.06 g cm⁻³ (measured using the undisturbed core method described by Blake and Hartge, 2006). Below 75 cm the sub-soil is heterogeneous, made up of saprolite, irregular granitic rock fragments embedded in a quartz-feldspar rich loam. The bulk density of the subsoil is 1.56±0.08 g cm⁻³. Soil chemical and physical properties are summarized in Table 1.

While the majority of cacao fine roots (diameter <2 mm) are predominantly concentrated at the soil surface (top 40 cm), the *Gliricidia* fine roots penetrate to greater depths (Moser et al., 2010). Fine roots of both tree species extended to a maximum depth of 2.4 m.

2.2 Experimental design

A stratified random design consisting of six plots in a one hectare area was used in this experiment. Each plot was 40×35 m in dimension. Three control plots were left undisturbed while three treatment plots, hereafter called “roof plots”, were used to simulate drought conditions. In the roof plots we built a transparent roof below the plantation canopy to divert throughfall away from the plot. The roof consisted of 1500 long and narrow bamboo frames (0.5×4.6 m) onto which transparent polyethylene plastic sheets were mounted. The roof was built at a height of approximately 1.2 m. Temperature, humidity and incident radiation under the panels were unaffected by the establishment of the roof. In March 2007, the roof was 60% closed, with small gaps located around the tree stems and between some panels. In January 2008, the roof closure was further increased to approximately 80%, by building smaller panels to close some of the bigger gaps. Runoff was diverted into a series of wooden, plastic lined gutters and channeled down-slope of the plot. Every two weeks leaf litter that accumulated on the roof panels was transferred back to the soil surface. Along the perimeter of each plot a 0.4 m trench was dug and lined with plastic to prevent lateral and surface water flows from entering the plots.

Table 1. Soil physical and chemical characteristics of the cacao agroforestry site in Sulawesi, Indonesia.

Sampling depth (cm)	Bulk density (g cm ⁻³)	Soil Texture			Carbon (g kg ⁻¹)	Nitrogen (g kg ⁻¹)	ECEC (cmol kg ⁻¹)	Soil pH (H ₂ O)
		Sand (%)	Silt (%)	Clay (%)				
Control Plots								
-5	1.27±0.02	60.7±1.7	25.7±0.2	13.6±1.6	16.6±1.4	1.5±0.1	7.7±1.3	5.8±0.3
-10	1.31±0.01	54.1±1.8	31.1±2.4	14.8±1.3	10.7±1.3	1.0±0.1	6.6±0.6	5.6±0.1
-20	1.33±0.02	55.1±1.0	28.3±0.9	16.5±0.5	6.4±0.1	0.6±0.0	7.3±1.3	5.9±0.3
-40	1.31±0.02	53.9±0.0	25.5±1.2	20.6±1.2	4.2±0.3	0.4±0.0	5.3±0.8	5.7±0.0
-75	1.36±0.08	58.6±2.8	22.2±2.6	19.2±1.8	3.4±0.3	0.4±0.0	7.5±1.9	5.9±0.0
Roof Plots								
-5	1.23±0.02	59.6±0.9	28.4±1.8	12.1±2.7	16.3±2.4	1.6±0.2	9.9±1.2	6.0±0.1
-10	1.26±0.02	55.9±1.1	28.2±1.8	16.0±1.1	14.5±2.9	1.3±0.2	9.0±0.3	6.4±0.1
-20	1.30±0.00	56.2±3.0	28.1±2.6	15.6±0.4	7.7±1.1	0.7±0.1	7.9±0.1	6.3±0.0
-40	1.32±0.04	56.1±1.7	27.4±2.6	16.6±1.6	4.6±0.1	0.4±0.0	5.6±0.2	6.0±0.1
-75	1.37±0.01	57.3±1.2	23.4±1.5	19.3±0.9	3.3±0.2	0.4±0.0	7.9±2.5	5.8±0.3

Notes: mean value (± 1 SE); *n* = 3.

ECEC: effective cation exchange capacity.

All measurements were made within a “core zone” (30×25 m) in the plot, leaving a 5 m buffer zone along the inside of the plot boundary to avoid edge effects. Per plot one central soil pit (0.8 m width × 1.6 m length × 3.0 m depth) was dug and equipped with gas samplers, thermocouples and soil moisture probes. Three parallel transects per plot were set up within the “core zone” for soil CO₂ flux measurements.

The experiment began in late January 2007, one month prior to the roof closure in the treatment plots. Pre-treatment measurements were made to verify that control and roof plots did not exhibit any initial systematic differences. The roof was closed at the beginning of March 2007 and remained closed for 13 months. The roof was opened in mid April 2008 and measurements continued for an additional five months to monitor the recovery of the ecosystem.

2.3 Soil surface CO₂ efflux measurements

We determined the soil surface CO₂ efflux (soil respiration) using dynamic closed chambers (Parkinson, 1981; Norman et al., 1992). At each plot, two circular polyvinyl chloride (PVC) chamber bases (0.045 m² area, 0.15 m height) were set up in each of the three parallel transects. In total six chambers were established per plot. In the roof plots, chamber bases were located under a range of roof closure conditions ranging from tightly closed to relatively open with more gaps. The chambers were established between 1.1 and 2.1 m from the nearest tree. During installation, chamber bases were embedded 1–2 cm into the soil surface. Prior to each measurement we removed all emergent vegetation from inside the chamber base and fanned the air above the chamber for at least one minute in order to bring the soil surface CO₂ concentrations to near atmospheric concentra-

tions. We also measured the chamber height at three places around the chamber base in order to get a good estimate of air volume within the chamber headspace. Measurements entailed attaching a chamber hood (12 cm height) tightly to the chamber base. Air in the headspace was subsequently circulated by a small battery-operated pump at a rate of 0.8 L min⁻¹ between the chamber and an infrared CO₂ gas analyzer (IRGA) (LI-800; Li-Cor Inc., Lincoln, NE, USA). The chamber was closed for 5 min 30 s. Atmospheric pressure was maintained within the chamber during measurements by using a small metal vent (0.1 cm diameter and 2.5 cm length) installed on top of the chamber hood. Carbon dioxide concentrations were recorded every 5 s using a datalogger (Campbell CR800). A two point calibration of the infrared CO₂ gas analyzer was done in the laboratory between sampling expeditions. The first point calibration was with a “zero” standard gas, which was created by removing CO₂ from the air by running air in a loop through a scrubber column of soda lime (4–8 mesh). The second point calibration was made using a CO₂ standard gas (700 ppm, Deuste Steininger GmbH, Mühlhausen, Germany), while a third CO₂ standard gas (356 ppm, Deuste Steininger GmbH, Mühlhausen, Germany) was used to test the quality and accuracy of the calibration.

Soil respiration flux was calculated from a 2.5 min time window during which CO₂ concentrations increased linearly; the coefficient of determination (*R*²) usually exceeded 0.993. Simultaneous to CO₂ efflux sampling we measured soil and air temperature with a handheld electronic thermometer (Greisinger GMH 3210) with a 12 cm measurement probe. Soil moisture was also measured using a portable TDR (time domain reflectometry) (Campbell Scientific Hydrosense – CS620) unit at 3 points around the chamber base. Measurements were made every two weeks between 08:00 a.m. and

05:00 p.m. The sequence in which plots were measured was randomized during each sampling expedition to minimize effects from diurnal fluctuations. In total, 36 soil respiration measurements were made per sampling expedition using the portable infrared CO₂ gas analyzer. During the experimental period we carried out 47 sampling expeditions. Due to an equipment failure with the IRGA we did not measure soil respiration in August 2007.

To study the contribution of leaf litter to CO₂ efflux, we randomly selected two experiment chambers in each control plot (in total 6 chambers). At each of the selected chambers, two additional chambers were installed directly adjacent to the “main” chamber (<1 m away). We removed litter from one chamber and placed it into the second chamber. The “main” chamber was left undisturbed and used as a control. The differences in CO₂ efflux between the three chambers were compared. The CO₂ produced from the litter layer was calculated by subtracting the CO₂ flux respired by the “main” chamber from that respired by the litter-removed chamber. Measurements were made during 36 sampling expeditions.

2.4 Soil air CO₂ concentrations and soil moisture depth profiles

Gas samples for CO₂ concentration analyses were collected from one central soil pit per plot. Samples were taken bi-weekly in conjunction with soil respiration measurements. The gas samplers consisted of thin stainless-steel tubes (1 mm inner diameter), where one end was perforated with small holes and the other end was fitted with an airtight septum holder. The samplers were inserted horizontally into the soil profile at 10, 20, 40, 75, 150 and 250 cm depths. Samplers in the top 75 cm were 1 m in length, while the samplers inserted at greater depths (150 and 250 cm) were slightly longer (1.5 m) to take into consideration the diffusion losses near the soil pit wall. Each sampler was equipped with a thermocouple (Type K) at its tip so that temperature could be recorded at the time of sampling with a handheld unit (Greisinger GMH 3210). Before taking a gas sample, 5 mL of air was extracted and discarded to clear the sampler of any stagnant “dead” air. We took the gas samples by connecting a pre-evacuated, air-tight glass vial (50 mL) to the sampler’s septum holder with a syringe needle and short flexible plastic tube. A two-way stop valve on the glass vial was then opened to suck in the gas sample. A sample was also taken at the soil surface by sticking a polypropylene syringe (with 5 cm needle) into the ground and drawing a sample.

Samples were analyzed in a laboratory at Tadulako University in Palu, Sulawesi, within 72 h after collection in the field. We measured the CO₂ concentration of each sample using a gas chromatograph (GC) (GC-11, Delsi Instruments, Suresnes, France) with thermal conductivity detector (TCD). Sample CO₂ concentrations were calculated by comparing the integrated peak areas to that of two known standard gas

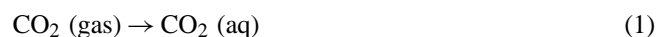
concentrations (0.07% and 3.5%, Deuste Steininger GmbH, Mühlhausen, Germany), to make a two point calibration.

In addition to the CO₂ concentration and temperature measurements, volumetric soil water content was also measured using TDR sensors (Campbell CS616) in three soil pits per plot. TDR sensors were installed adjacent to each gas sampler, in the central pit, by inserting them into the undisturbed soil at the end of a 30 cm hole dug horizontally into the soil pit wall. Soil moisture was recorded hourly using a datalogger (Campbell CR1000). Due to high rock content we could not install TDR sensors in three plots at 250 cm depth. Using undisturbed soil samples we calibrated the water content measurements using the methodology described by Veldkamp and O’Brien (2000). Volumetric water content was recalculated to soil matric potential using soil water retention curves developed by van Straaten (unpublished data).

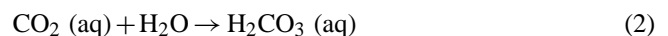
Soil CO₂ concentration measurements were made during 46 field sampling expeditions, in conjunction with the IRGA soil respiration measurements. One additional was missed due to a large landslide that limited access to the site with the gas sampling equipment.

2.5 CO₂ leaching losses

The downward CO₂ leaching flux was determined by multiplying the amount of CO₂ dissolved in water with modeled drainage rate estimates. According to Henry’s Law, CO₂ dissolved in water is proportional to the partial pressure of CO₂ above the solution and the CO₂ Bunsen absorption coefficient. When CO₂ dissolves into water it can produce two possible reactions (Eqs. 1 and 2). The solubilization of CO₂ gas:



and hydration of CO₂ (aq) to form carbonic acid



However, given the low proportion of H₂CO₃ (aq) relative to CO₂ (aq) it is possible to lump their concentrations together with Henry’s Law. The dissolved CO₂ was calculated as follows:

$$M\text{-CO}_2w = \text{CO}_2a \times \text{VWC} \times B \quad (3)$$

Where: *M-CO₂w* is the CO₂ content dissolved in the liquid phase (g CO₂ m⁻³), *CO₂a* is the partial pressure of CO₂ (concentration) in the soil air (g CO₂ m⁻³) at atmospheric air pressure, *VWC* is the soil’s volumetric water content and *B* is the Bunsen solubility coefficient for CO₂. The Bunsen coefficient is the volume of gas that can be absorbed by one cubic meter of water at standard atmospheric air pressure, at 24 °C, the CO₂ Bunsen coefficient is 0.7771 g m⁻³.

Dissolved CO₂ was calculated for the gas samples taken at 250 cm soil depth and interpolated to give daily values of dissolved CO₂ throughout the duration of the experiment.

Subsequently, dissolved CO₂ was multiplied with daily modeled soil water drainage to determine CO₂ leaching losses. Soil drainage from roof and control plots were modeled using HYDRUS 1-D (Šimnek et al., 2008) with measured transpiration rates, net precipitation and soil water contents as input. The method has been described in greater detail in Köhler (2010). Leaching losses were calculated only from 10 February, 2007 to 5 June, 2008 because of the shorter time frame in which soil water drainage was modeled.

2.6 Isotope analysis

To identify the origin of the high CO₂ concentrations in deep soil, ¹³CO₂ isotope signatures were measured. One soil air sample was taken from each plot at 250 cm depth, stored in airtight, stainless steel vials and transported to the Center for Stable Isotope Research and Analysis (KOSI, Georg-August-University Göttingen, Germany) for analysis using a Isotope Ratio Mass Spectrometer (Finnigan MAT Delta Plus, Bremen, Germany).

2.7 Data analysis

We divided the experiment into four time periods. The first was the “pre-treatment period” which started on 27 January, 2007 and lasted until the roof was closed on 1 March, 2007 – a total of 33 days. The period of roof closure was subsequently divided into two periods, the first being the initial ten months when the drought effect was mild, hereafter referred to as treatment period #1 (from 1 March 2007 to 1 January 2008; 306 days), followed by treatment period #2, which corresponded to the time when the drought effect was more pronounced and ran until 10 April 2008 when the roof was opened (100 days). The fourth was the “post-treatment period” which extended until 27 August, 2009 (139 days). Throughout the experiment, roof plot measurements were compared to adjacent control plot measurements to decipher roof plot ecosystem drought response from normal fluctuations. Individual soil CO₂ efflux chamber measurements were averaged for each plot at each measurement date and logarithmically transformed to normalize data distributions. The significance of the drought effect difference was tested using linear mixed effects models for the four time periods mentioned above. In the model, the drought treatment was considered a fixed effect while the measurement day (from day 1 to day 579) and plot were considered random effects. Differences were considered significant if $P \leq 0.05$. Additionally, temporal autocorrelation in this time series CO₂ flux dataset was corrected for by using a first order autoregressive model.

We used a multiple linear regression analyses to establish predictive relationships between temporal soil CO₂ efflux, soil moisture and soil temperature. We stratified the data into three soil moisture classes: wet ($pF \leq 1.2$), intermediate ($1.2 < pF \leq 1.7$) and dry ($pF > 1.7$). Subsequently, for each

class we determined the variability of CO₂ efflux explained by the two variables (coefficient of determination). Correlation coefficients for soil temperature and soil moisture were determined to test the strength of the correlation between the two independent variables.

Additionally, to discern the extent of autotrophic respiration and belowground tree drought reactions, we tested how soil CO₂ efflux correlated with *Gliricidia* and cacao sap flux densities, solar radiation, and the chamber distance from adjacent trees respectively using simple linear regressions. All statistical analyses were done using the statistical package R version 2.8.1 (R Development Core Team, 2008).

3 Results

3.1 Volumetric soil water content and soil temperature

During the pre-treatment phase, volumetric soil water content of all six experiment plots were in the same range for each respective sampling depth (Fig. 1c). Approximately ten days after roof closure, soil water contents began to diverge between the control and roof plots. Soil moisture contents in the plots under the roof decreased simultaneously at all depths, apart from the depth of 250 cm which began drying out only after a period of two and a half months. Although gaps in the roof did allow some throughfall to enter, the water recharge was limited to the upper soil layers and was never sufficient to recharge the soil under roof to control plot levels. A natural drought in January–February 2008 reduced soil water contents in both roof and control plots. The drying effect was recorded down to 250 cm depth in the control plots. Minimum soil water contents in the roof plots were experienced during this dry spell. Upon roof opening in April 2008, soil water contents in the roof plots quickly rose to near control plot levels.

Soil surface temperature exhibited little fluctuation throughout the duration of the experimental period, ranging from a minimum temperature of 21.8 °C to a maximum temperature of 24.8 °C. The average soil temperature at 5 cm depth was unaffected by the roof installation, measuring 23.2 ± 0.8 °C and 23.0 ± 0.7 °C (mean \pm SD) for the roof and control plots respectively. At 250 cm depth, soil temperatures were slightly higher than at the surface and averaged 24.0 ± 0.4 °C (mean \pm SD).

3.2 Soil surface CO₂ efflux

Soil surface CO₂ efflux was highly variable in both space and time. Spatially, the average coefficient of variation of the 18 roof plot and 18 control plot chambers was 52% and 46% respectively over the period of the experiment. The temporal coefficient of variation for individual chamber measurements was slightly lower in the control plots (40%) in comparison to the treatment plots (53%).

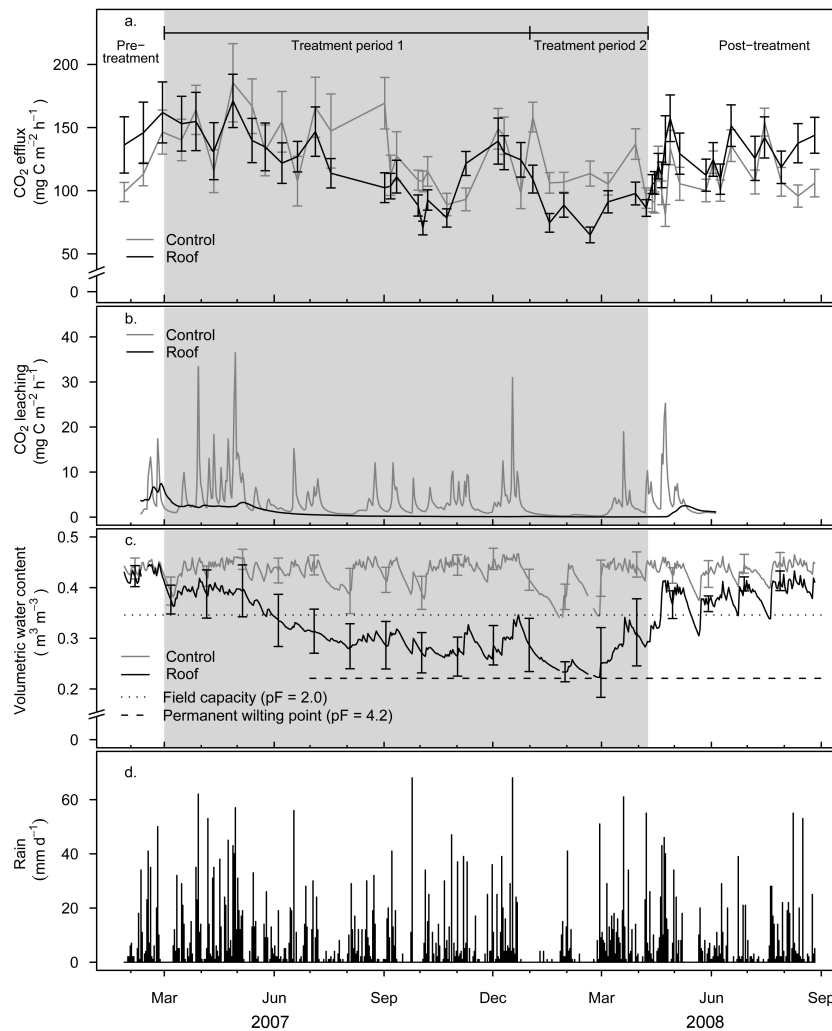


Fig. 1. (a) Average soil surface CO₂ efflux in control and roof plots, (b) average CO₂ leaching losses in control and roof plots, (c) average volumetric water content at 10 cm soil depth in control and roof plots and (d) daily precipitation. Error bars indicate ± 1 SE. The shaded area indicates the period of roof closure.

During the pre-treatment phase, soil CO₂ efflux measurements was not significantly different between roof and control plots (roof: 142.5 ± 32.9 mg C m⁻² h⁻¹, control: 118.0 ± 18.2 mg C m⁻² h⁻¹ (mean \pm standard error, $n = 3$)) (Fig. 1a). In the first ten months of the simulated drought (treatment period #1) soil CO₂ efflux treatment means did not deviate significantly (roof: 124.1 ± 8.5 mg C m⁻² h⁻¹, control: 136.9 ± 10.9 mg C m⁻² h⁻¹ (mean \pm standard error, $n = 21$)). The onset of a natural dry spell, combined with improved roof closure finally caused roof plot CO₂ efflux to drop significantly below the control for the remaining three months of the simulated drought (treatment period #2). During this time, soil respiration in the roof plots decreased by 26% ($P < 0.05$) in comparison to the control (roof: 85.5 ± 8.2 mg C m⁻² h⁻¹, control: 115.9 ± 9.9 mg C m⁻² h⁻¹ (mean \pm standard error, $n =$

7)). The overall difference in average soil CO₂ efflux between the control and the roof plots was relatively minor during the 13-month simulated drought. Soil CO₂ efflux declined only slightly (13%) in the roof plots in comparison to the control plots (roof: 119.5 ± 5.4 mg C m⁻² h⁻¹, control: 126.2 ± 5.4 mg C m⁻² h⁻¹ (mean \pm standard error, $n = 47$)).

Within three days of opening the roof, in April 2008, soil CO₂ efflux rose to control plot levels. No pronounced CO₂ efflux peak was measured and over the next five months the average roof plot CO₂ efflux did not significantly differ from the control (roof: 129.1 ± 13.6 mg C m⁻² h⁻¹, control: 111.9 ± 6.7 mg C m⁻² h⁻¹ (mean \pm standard error, $n = 16$)). One roof plot chamber was removed from the analysis shortly after roof opening as it suddenly began producing very high CO₂ fluxes.

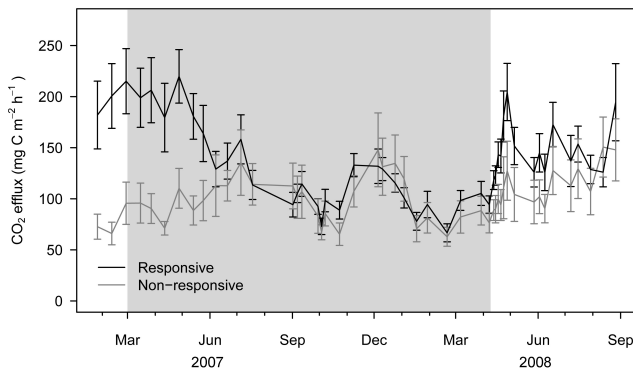


Fig. 2. Soil CO₂ efflux from drought responsive efflux chambers and non-responsive efflux chambers in the roof plots. Error bars indicate ± 1 SE. The shaded area indicates the period of roof closure.

The cumulative CO₂ respired from control and roof plots were not significantly different, indicating the drought had a CO₂ neutral effect. The cumulative CO₂ flux from the 579-day experiment was 17.5 ± 0.75 mg C ha⁻¹ and 16.6 ± 0.74 mg C ha⁻¹ for the control and roof plots respectively. Annually this equates to 11.1 ± 0.5 Mg C ha⁻¹ yr⁻¹ for the control plot and 10.5 ± 0.5 mg C ha⁻¹ yr⁻¹ for the roof plot.

Although the overall drought response in the roof plots was moderate, 11 of the 18 efflux chambers in the roof plots exhibited stronger drought effects than the others (Fig. 2). Drought effects were most pronounced at chamber sites already producing high CO₂ before the roof closure. We used the coefficient of determination (R^2) of a linear regression between CO₂ efflux and the soil moisture as an index of drought response (hereafter called the “drought response index”) and plotted it spatially (Fig. 3). The drought response appeared to be localized, as some chamber sites measured strong relationships to soil water content changes (up to $R^2 = 0.70$), while other chambers located nearby measured little to no response to decreasing soil water contents.

Over the course of the 19-month measurement period, no distinguishable seasonal patterns in either precipitation (Fig. 1d) or in air temperature were measured (data not shown).

3.3 Controls regulating CO₂ efflux

Soil CO₂ efflux exhibited a strong relationship with soil moisture. CO₂ efflux peaked under intermediate soil moisture contents (between pF 1 and 2) and decreased when conditions became either wetter ($R^2 = 0.34$, $p < 0.01$), or drier ($R^2 = 0.71$, $p < 0.01$) (Fig. 4). The rate of change (slope) at the wet end of the moisture spectrum was steeper than at the drier end. At the wet end of the moisture spectrum (pF ≤ 1.2), soil moisture accounted for 39% of the CO₂ efflux variation, while soil temperature accounted for 9% ($P < 0.01$). At intermediate soil moisture ($1.2 < \text{pF} \leq 1.7$) neither soil tempera-

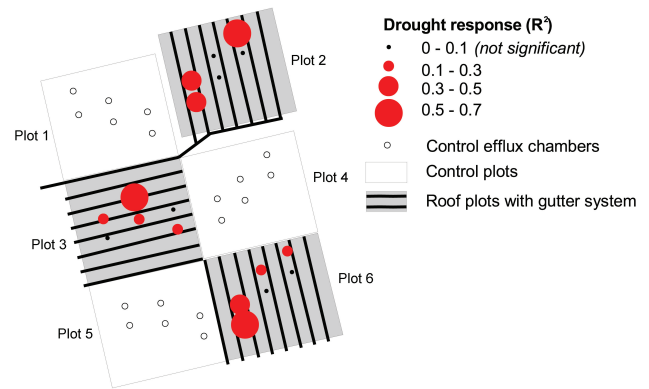


Fig. 3. Schematic of cacao agroforestry plot layout and response of CO₂ flux chambers to soil water content changes. The coefficient of determination (R^2) for the CO₂ efflux to volumetric water content was used as an index of how strong a chamber reacted to changes in soil moisture.

ture nor soil moisture could explain the variability exhibited in CO₂ efflux. Lastly, under dry conditions (pF > 1.7) soil moisture accounted for 73% ($P < 0.01$) of the CO₂ efflux variation while the soil temperature influence was insignificant. Soil moisture and soil temperature were not correlated at any of the three soil moisture categories.

A weak diurnal pattern was detected in soil respiration in the control plots, whereby CO₂ efflux was lowest early in the early morning between 06:00 a.m. and 08:00 a.m. (107.6 ± 12.6 mg C m⁻² h⁻¹) and rose steadily throughout the day reaching a maximum in the mid-afternoon between 02:00 and 04:00 p.m. (142.0 ± 8.6 mg C m⁻² h⁻¹, mean ± 1 SE).

Soil respiration was found to decrease with distance from cacao tree stems ($R^2 = 0.22$, $P < 0.01$), but showed no relationship with distance from *Gliricidia* trees. In the roof plots, the CO₂ drought response index declined with distance from cacao tree stems ($R^2 = 0.23$, $P = 0.053$), but showed no relationship with distance to *Gliricidia* tree stems.

3.4 Leaf litter respiration

The leaf litter layer contributed on average 16.8% of the total respired CO₂ efflux. Although we did not measure the moisture of the litter layer directly there is a strong indication that respiration rates were positively related to the moisture regime of the leaf litter. Soil moisture probes located at 10 cm soil depth showed a positive linear relationship ($R^2 = 0.20$, $P < 0.01$) between soil moisture and the leaf litter CO₂ efflux contribution. In other words, when conditions were dry CO₂ efflux from the litter was low and did not contribute much to the overall soil flux (~ 3 –4% of the total flux). However, when conditions were wet, leaf litter CO₂ efflux increased and became an important CO₂ production source contributing up to 40% of the overall CO₂ efflux. The leaf litter CO₂

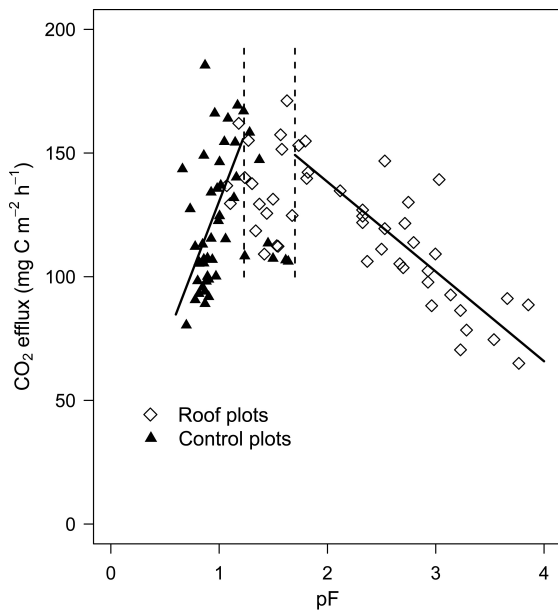


Fig. 4. Relationship between soil water potential (pF) at 10 cm depth and soil CO₂ efflux. The regression equation at the wet end of the moisture spectrum is $\text{CO}_2 \text{ efflux} = 114.35(\text{pF}) + 16.13$ ($R^2 = 0.34$, $P > 0.01$) and at the dry end $\text{CO}_2 \text{ efflux} = -36.26(\text{pF}) + 210.86$ ($R^2 = 0.71$, $P > 0.01$).

contribution to the overall control plot CO₂ flux over the duration of experiment is shown in Fig. 5.

3.5 Soil profile CO₂ concentrations

Soil CO₂ concentrations increased with soil depth, displaying an exponential shape in concentration rise. CO₂ concentrations near the soil surface (0–10 cm) were relatively low and increased rapidly with depth (between 20–75 cm depth) and approached an asymptote at deeper soil depths (150–250 cm). The average CO₂ concentration at 250 cm depth was 11.8% in the control plots over the duration of the experiment. This is more than 300 times higher than atmospheric CO₂. The highest recorded CO₂ concentration was 15.3% in October 2007 in one of the control plots.

During the pre-treatment period, soil CO₂ concentrations in the control and treatment plots were similar for each respective soil depth (Fig. 6). Upon roof closure, CO₂ concentrations in the roof plots began to decline in conjunction with the drying out of the soil profile. Carbon dioxide concentrations declined steadily over the 13-month treatment period and reached a minimum level in the last month of the induced drought. In comparison to the control plots, roof plot soil CO₂ concentrations decreased by up to 83% at 10 cm depth and up to 48% at 250 cm depth. During the driest period of the simulated drought (treatment period #2) the soil CO₂ concentration depth profile was nearly linear in shape, supposedly saturating at a deeper depth than from which we

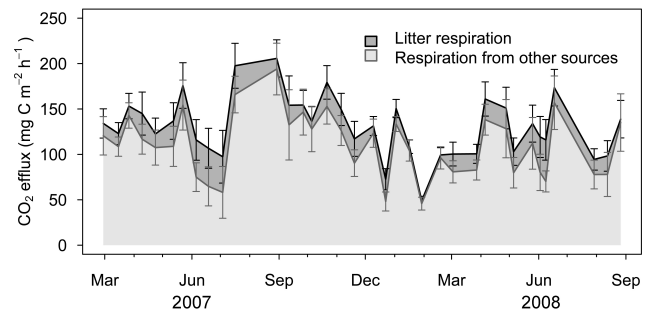


Fig. 5. CO₂ efflux from leaf litter contribution study in the control plots. The dark grey color indicates the CO₂ production derived from leaf litter, while the light grey color denotes the CO₂ production from within the soil profile from other sources. The error bars indicate the standard error of the six measurements per sampling date.

sampled. Although CO₂ concentrations in the control plots remained relatively constant throughout the treatment period, a sharp drop was measured at all soil depths in January–February 2008, during a phase of natural drought. When we opened the roof in April 2008, CO₂ concentrations rose quickly; within a one month period CO₂ concentrations at all depths rose to near control plot levels whereby CO₂ concentrations at shallower depths rose faster than in the subsoil. Thereafter, CO₂ concentrations leveled off, and remained lower than the control plot until the end of the experiment in August 2008.

The $\delta^{13}\text{C}$ isotope signature of the six CO₂ gas samples was $-23.6 \pm 0.19\text{‰}$ (mean \pm SD) indicating that the CO₂ present in the soil profile is biologically produced and most likely produced by C₃ plants – e.g. cacao and *Gliricidia*.

3.6 CO₂ leaching losses

In the control plots, 93% of the total carbon dioxide was stored in soil water as aqueous CO₂ while the remaining 7% was present in the gaseous phase. In the roof plots, on average 65% of the total CO₂ was dissolved in soil water.

Dissolved CO₂ drainage losses during the experiment are shown in Fig. 1b. In the control plots, CO₂ leaching losses spiked during periods of high drainage. They reached as high as $36.5 \text{ mg C m}^{-2} \text{ h}^{-1}$ (15% of the total CO₂ flux), on a single day. However, on average the CO₂ drainage in the control plots remained low at $3.5 \text{ mg C m}^{-2} \text{ h}^{-1}$, which is 2.6% of the overall surface flux. In the roof plots, CO₂ leaching was even lower given the drier soil profile and reduced drainage discharge. During the treatment period, soil water drainage approached zero. In these plots the CO₂ leaching losses were on average $0.82 \text{ mg C m}^{-2} \text{ h}^{-1}$.

4 Discussion

4.1 CO₂ fluxes in a cacao agroforestry system

As far as we are aware, this study represents the first in situ measurements of soil CO₂ dynamics of a cacao agroforestry ecosystem. Measured CO₂ efflux rates indicate that the ecosystem is very productive as respiration rates were within or slightly below the range measured in tropical forest ecosystems in Asia (Adachi et al., 2006; Ohashi et al., 2008), and in Latin America (Davidson et al., 2000, 2008; Schwendenmann et al., 2003; Sotta et al., 2006).

The main controlling variable driving temporal variation in soil CO₂ efflux in this ecosystem was soil moisture. Soil respiration peaked at intermediate soil water contents and declined under both wetter and drier conditions (Fig. 4). Unlike the gradual decline observed in soil respiration when conditions got drier (as was observed in the roof plots and will be discussed later), soil respiration rates in the control plots often plummeted when moist soil became slightly wetter. This is evident by the steep slope shown at the wet end of the moisture spectrum in Fig. 4. As a result, the CO₂ flux in the control plots exhibited strong efflux fluctuations with minor changes in soil moisture. The reduction in soil CO₂ efflux under the saturated conditions may be a result of a diffusion block that prevented CO₂ from exiting the soil through the saturated pore space, and/or prevented oxygen from diffusing into the soil – subsequently creating anaerobic conditions (Luo and Zhou, 2006).

CO₂ production from the leaf litter was sensitive to moisture conditions. When external conditions were wet the litter layer contributed as much as 40% of the total CO₂ efflux, however when conditions were dry, the CO₂ contributions from the litter layer was nearly zero percent.

Soil temperature displayed a slightly positive relationship with soil CO₂ efflux at the wet end of the soil moisture spectrum. The temperature influence, however, was very minor given the small temperature variation (in total 3 °C) experienced during the 19-month experimental period. In contrast to studies conducted in rainforests in the Amazon basin (Wofsy et al., 1988) and in Costa Rica (Schwendenmann et al., 2003), the effect of solar radiation on plant photosynthesis was not observed in the soil respiration measurements for this site.

Dissolved CO₂ leaching beyond 250 cm soil depth proved to be only a minor CO₂ flux (Fig. 1b). Considering the high proportion of CO₂ stored in the liquid phase, the overall CO₂ leaching flux from below 250 cm was relatively low (3.5 and 0.8 mg C m⁻² h⁻¹ for control and roof plots respectively). This is in line or slightly higher than CO₂ leaching fluxes reported by studies in tropical forests in Latin America (Johnson et al., 2008; Schwendenmann and Veldkamp, 2006). The diffusion of CO₂ through soil water along the CO₂ concentration gradient is considered negligible since liquid phase

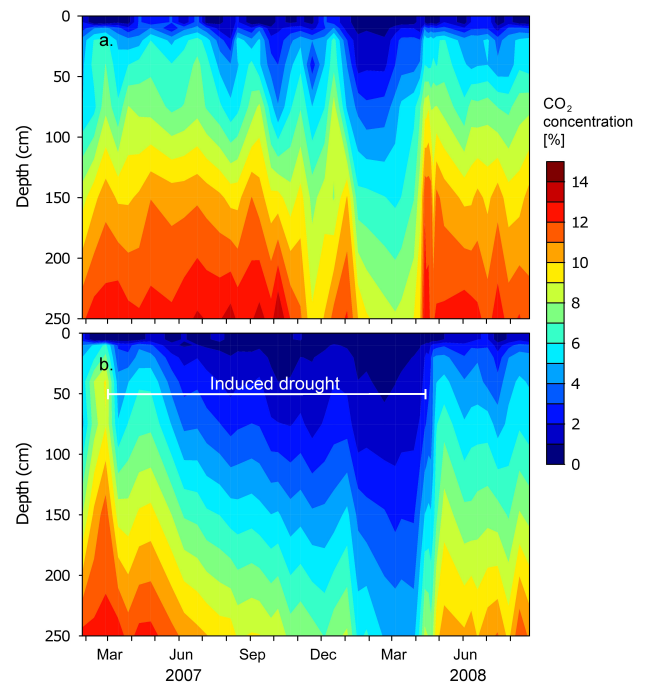


Fig. 6. Isoleths of average soil CO₂ concentrations (percent) in the soil profile of (a) control plots and (b) roof plots in soil air throughout the drought experiment.

diffusion (in free water) is more than 8000 times slower than CO₂ transport through free air (Moldrup et al., 2000).

4.2 Drought effects on soil CO₂ efflux

Since pre-treatment soil CO₂ efflux averages did not significantly differ between control and roof plots, subsequent differences exhibited during the period of roof closure are attributed to ecosystem drought responses. Though soil CO₂ efflux drought effects were not significantly different during the first 10 months (treatment period #1), a natural dry spell (and improved roof closure) in early 2008 was pivotal in causing significant CO₂ efflux declines in the following three months (treatment period #2). The decreases in soil CO₂ efflux coincided with drought stress symptoms exhibited in both cacao and *Gliricidia* trees (Schwendenmann et al., 2010).

In contrast to our initial hypotheses, the cacao agroforestry system exhibited only a mild CO₂ efflux response to the induced drought. The moderate 13% decrease in soil CO₂ efflux experienced during the induced drought in the roof plots can be attributed to a number of factors. The soil moisture relationship with soil CO₂ efflux obscured differences between control and roof treatments. Since soil respiration peaked at intermediate soil moisture and was low under both wet and dry conditions (Fig. 4), it meant that respiration differences between control and roof plots were masked when soil moisture conditions were concurrently very wet in the control and

dry in roof plots. However, unlike the control plots where slightly wetter conditions caused soil respiration to decrease rapidly, the drying process observed in the roof plots caused a slow decrease in soil respiration (evident by the gradual slope at the dry end of the moisture spectrum in Fig. 4).

We have several indirect indications that different CO₂ sources reacted differently to drought stress. The first indirect indication comes from the spatial variability of soil respiration across the project area. While eleven efflux chamber sites in the roof plots showed relatively strong declines in soil CO₂ efflux as the soil dried out, the other seven efflux chambers, often just a few meters away, exhibited little to no reaction (Fig. 2 and Fig. 3). This localized drought response is indicative of the contrasting processes taking place directly below the respective chambers. Under some chambers soil respiration was dominated by CO₂ production sources sensitive to moisture stress (under responsive chambers), i.e. root respiration, while under other chambers the CO₂ efflux was dominated by sources more resilient to drier conditions (non-responsive chambers) i.e. soil micro-organism respiration. The second indirect indication was that soil CO₂ efflux from chambers that exhibited strong drought response correlated closely to the sap flux ratios of both cacao ($R = 0.61$, $P < 0.01$) and *Gliricidia* trees ($R = 0.65$, $P = 0.01$) as reported by Schwendenmann et al. (2010). In contrast, those chambers that did not exhibit a drought sensitive CO₂ efflux did not correlate significantly with sap flux density. Although this does not necessarily establish a causal relationship between soil CO₂ efflux and tree sap flux, it does show that when tree metabolisms slowed down, CO₂ efflux corresponding decreased in the drought responsive efflux chambers. Our interpretation is that these drought responsive chambers, which had higher than average respiration rates even during the pre-treatment measurements, were situated above active roots and the onset of drought conditions induced tree drought stress which resulted in root respiration decreases. This is substantiated by the strong correlation between the average soil respiration prior to roof closure (pre-treatment) and the drought response index ($R^2 = 0.76$, $P < 0.01$, $n = 18$). This means that the high flux chambers were situated above already active CO₂ production sources, very likely active roots, which were susceptible to drought stress.

Furthermore, the drought effect on autotrophic respiration was again detected when examining the relationship between soil CO₂ efflux and the distance to tree stems. We found that the drought response index declined with distance from cacao tree stems suggesting that cacao rooting activity near the stem declined during the induced drought, while further away the effect was not as pronounced. We also found that average soil CO₂ respiration rates declined with distance from cacao tree stems in both control and roof plots. Soil compaction was excluded as a potential explanatory variable for these decreases, as bulk density cores taken at 0.25 m distance intervals outward from the tree stem to a maximum dis-

tance of 1.75 m, failed to show any systematic increases with distance ($n = 6$ cacao trees). Stem flow and the potentially wetter conditions around the tree base was also excluded as an explanatory variable as we did not find an evident relationship between the average soil moisture and the respective distance to the tree.

Unlike the cacao trees, we did not observe similar tree distance relationships with *Gliricidia* trees. This is thought to be primarily due to the deeper and more diffuse root architecture and rooting behavior exhibited by *Gliricidia* fine roots (Moser et al., 2010), which may have masked measurable effects with distance. A Deuterium (δD) study by Schwendenmann et al. (2010) found that tree water uptake was partitioned vertically in the soil horizon, where cacao accessed water from the upper horizons while *Gliricidia* explored for water in deeper soil layers.

Additionally, a root excavation exercise done by Moser et al. (2010) at the site, found that coarse roots of both cacao and *Gliricidia* were primarily concentrated around the tree stems while fine root (diameter < 2 mm) distributions extended well into the agroforestry plantation. Other studies by Harteveld et al. (2008) and Kummerow et al. (1982) confirm that cacao fine roots extend well beyond the stem and are primarily concentrated in the uppermost 30 cm. Although overall autotrophic respiration rates appeared to decline, Moser et al. (2010) reported that cacao and *Gliricidia* fine root biomass remained unchanged at all soil depths to 250 cm, over the duration of the 13-month induced drought. These findings suggest that regardless of the drought stress the trees still continued to maintain and build new fine roots required to search for available water resources.

The litter layer, as was previously mentioned, is sensitive to changes in moisture regimes. Therefore, given that the litter layer would have dried out relatively quickly, the effect on soil respiration would have also been correspondingly fast. By the end of the roof experiment, in April 2008, visibly more leaf litter was found on the plantation floor of the roof plots than the control, although leaf litter fall was unaffected by the induced drought (Schwendenmann et al., 2010). This is an additional indication that decomposition rates decreased under the drier conditions.

Although we have little data to substantiate how below-ground heterotrophic CO₂ respiration from soil microorganisms in the bulk soil reacted to the drought, the results from the leaf litter study clearly show that heterotrophic respiration was sensitive to droughts.

4.3 Belowground CO₂ dynamics

Baseline carbon dioxide concentrations in deep soil air were among the highest ever reported for soils (Davidson et al., 2006; Schwendenmann and Veldkamp, 2006; Sotta et al., 2007). The average CO₂ concentration at 250 cm soil depth in the control plots was 11.8%, and peaked at 15.3%, during the 19-month experiment. The $\delta^{13}C$ isotope signature

of the sampled soil air CO₂ (−23.6‰) confirmed that the CO₂ produced originated from plants having a C₃ photosynthetic pathway. Since soil CO₂ diffusion typically leads to enrichment of 4.4‰ (Amundson et al., 1998), the resulting −28‰ clearly falls in the δ¹³C signature range produced by C₃ plants (between 22‰ and −34‰) (Trumbore and Druffel, 1995). This excludes that the CO₂ came from either geological origins (δ¹³C signature of carbonate rocks is between 0‰ and +5‰) or from C₄ plants (δ¹³C signature between −10‰ and −20‰).

The high CO₂ concentrations in soils of the cacao agroforestry ecosystem are thought to be caused by a diffusion block that prevented CO₂ molecules from traveling upward along the concentration gradient to the atmosphere. Gaseous CO₂ diffusion was slowed down by the soil medium's high bulk density (low porosity), high concentration of coarse rock fragments as well as soil water. Each of these components would have increased the tortuosity of the gas pathway to the soil surface. During wet conditions CO₂ concentrations were high in the soil air, as the pore-space would have been saturated with water and resulted in slow diffusion. However, as soon as the soil dried out, the CO₂ concentrations began to decline, as there were more open air filled pore-spaces available for CO₂ diffusion. This trend is apparent in both the roof plots (where we artificially manipulated the soil moisture) and in the control plots during a natural drought in January–February 2008 (Fig. 6). In and of itself, the soil air CO₂ concentrations do not say very much about the soil carbon allocation dynamics, but highlight the CO₂ storage capacity of the soil.

4.4 Rewetting phase

Soil CO₂ efflux levels rose almost immediately after the first rain showers began to rewet the soil profile. Within three days, soil CO₂ efflux reached control plot levels and remained at par with it for the remaining five months. We attribute the quick recovery to the mineralization of dead accumulated labile organic matter that became wet. The unexpected lack of a pronounced rewetting peak thereafter may be due to: 1) increased hydrophobicity of organic particles which in turn affected decomposition rates (Goebel et al., 2005), and/or 2) the ecosystem's adaptation to drying and wetting cycles, where a quick response and recovery indicates that the ecosystem is well adapted to drying and rewetting (Borken and Matzner, 2009). Indications of hydrophobicity are evident in the post-treatment period (Fig. 1c), where soil moisture failed to return to control plot levels despite frequent precipitation events and sufficient water to rewet the soil (monthly average of 225 mm over five months). The latter explanation can be partially substantiated by the rapid recuperation of sap flux densities in both cacao and *Gliricidia* trees after roof opening (Schwendenmann et al., 2010).

5 Conclusions

Although there were evidently some drought induced carbon responses, the net emission of soil CO₂ over the duration of the 19-month experiment remained unaffected. The 13-month simulated drought caused a slight decrease in soil respiration because of localized changes in root activity and declines in decomposition rates both above and belowground. The moderate soil CO₂ efflux decrease experienced during the drought indicates that this agroforestry ecosystem is capable of mitigating drought stress for extended periods.

Acknowledgements. The project was financed by the Deutsche Forschungsgemeinschaft (DFG) in the framework of the collaborative German-Indonesian research project SFB-552, sub-project B6. The authors gratefully acknowledge Purwanto for his assistance with the fieldwork, Luitgard Schwendenmann for her useful advice with data analysis, Kendra Leek for her help polishing the English, and Andreas Schindlbacher and two anonymous reviewers for their constructive reviews and suggestions.

Edited by: G. Wohlfahrt



This Open Access Publication is funded by the University of Göttingen.

References

- Adachi, M., Bekku, Y. S., Rashidah, W., Okuda, T., and Koizumi, H.: Differences in soil respiration between different tropical ecosystems, *Appl. Soil Ecol.*, 34, 258–265, 2006.
- Amundson, R., Stern, L., Baisden, T., and Wang, Y.: The isotopic composition of soil and soil-respired CO₂, *Geoderma*, 82, 83–114, 1998.
- Bailey, N. J., Motavalli, P. P., Udawatta, R. P., and Nelson, K. A.: Soil CO₂ emissions in agricultural watersheds with agroforestry and grass contour buffer strips, *Agroforest. Syst.*, 77, 143–158, doi:10.1007/s10457-009-9218-x, 2009.
- Blake, G. R. and Hartge, K. H.: Bulk density, in: *Methods of Soil Analysis. Part 1. Physical and Mineralogical Methods*, edited by: Klute, A., Soil Science Society of America, Madison, 2006.
- Borken, W. and Matzner, E.: Reappraisal of drying and wetting effects on C and N mineralization and fluxes in soils, *Glob. Change Biol.*, 15, 808–824, doi:10.1111/j.1365-2486.2008.01681.x, 2009.
- Davidson, E. A., Verchot, L. V., Cattânio, J. H., Ackerman, I. L., and Carvalho, J. E. M.: Effects of soil water content on soil respiration in forests and cattle pastures of eastern Amazonia, *Biogeochemistry*, 48, 53–69, 2000.
- Davidson, E. A., Yoko Ishida, F., and Nepstad, D. C.: Effects of an experimental drought on soil emissions of carbon dioxide, methane, nitrous oxide in a moist tropical forest, *Glob. Change Biol.*, 10, 718–730, 2004.

- Davidson, E. A., Savage, K. E., Trumbore, S. E., and Borken, W.: Vertical partitioning of CO₂ production within a temperate forest soil, *Glob. Change Biol.*, 12, 944–956, 2006.
- Davidson, E. A., Nepstad, D. C., Yoko Ishida, F., and Brando, P. M.: Effects of an experimental drought and recovery on soil emissions of carbon dioxide, methane, nitrous oxide, and nitric oxide in a moist tropical forest, *Glob. Change Biol.*, 14, 2582–2590, 2008.
- FAO: Food and Agriculture Organization of the United Nations, online available at: <http://faostat.fao.org>, (last access: November 2009), 2009.
- Goebel, M. O., Bachmann, J., Woche, S. K., and Fischer, W. R.: Soil wettability, aggregate stability, and the decomposition of soil organic matter, *Geoderma*, 128, 80–93, doi:10.1016/j.geoderma.2004.12.016, 2005.
- Harteveld, M. A., Hertel, D., and Leuschner, C.: Spatial and temporal variability of fine root abundance and growth in tropical moist forests and agroforestry systems (Sulawesi, Indonesia), *Ecotropica*, 13, 111–120, 2008.
- Hergoualc'h, K., Skiba, U., Harmand, J. M., and Henault, C.: Fluxes of greenhouse gases from Andosols under coffee in monoculture or shaded by *Inga densiflora* in Costa Rica, *Biogeochemistry*, 89, 329–345, doi:10.1007/s10533-008-9222-7, 2008.
- Johnson, M. S., Lehmann, J., Riha, S. J., Krusche, A. V., Richey, J. E., Ometto, J. P. H. B., and Couto, E. G.: CO₂ efflux from Amazonian headwater streams represents a significant fate for deep soil respiration, *Geophys. Res. Lett.*, 35, L17401, doi:10.1029/2008GL034619, 2008.
- Keil, A., Zeller, M., Wida, A., Sanim, B., and Birner, R.: What determines farmers' resilience towards ENSO-related drought? An empirical assessment in central Sulawesi, Indonesia, *Clim. Change*, 86, 291–307, doi:10.1007/s10584-007-9326-4, 2008.
- Köhler, M.: Cacao agroforestry under ambient and reduced throughfall: Tree water use characteristics and soil water budgeting, Ph.D., Faculty of Forest Sciences and Forest Ecology, Georg-August University of Göttingen, Göttingen, 140 pp., 2010.
- Kummerow, J., Kummerow, M., and Souza da Silva, W.: Fine-root growth dynamics in cacao (*Theobroma cacao*), *Plant Soil*, 65, 193–201, 1982.
- Luo, Y., and Zhou, X.: *Soil Respiration and the Environment*, Academic Press, Burlington, San Diego, London, 2006.
- Moldrup, P., Olesen, T., Schjønning, P., Yamaguchi, T., and Rolston, D. E.: Predicting the gas diffusion coefficient in undisturbed soil from soil water characteristics, *Soil Sci. Soc. Am. J.*, 64, 94–100, 2000.
- Moser, G., Leuschner, C., Hertel, D., Hölscher, D., Köhler, M., Leitner, D., Michalzik, B., Prihastanti, E., Tjitrosemito, S., and Schwendenmann, L.: The drought response of cocoa trees (*Theobroma cacao*) to a 13-month desiccation period in Sulawesi, Indonesia, *Agroforest. Syst.*, in press, 2010.
- Nepstad, D. C., Decarvalho, C. R., Davidson, E. A., Jipp, P. H., Lefebvre, P. A., Negreiros, G. H., Dasilva, E. D., Stone, T. A., Trumbore, S. E., and Vieira, S.: The role of deep roots in the hydrological and carbon cycles of Amazonian forests and pastures, *Nature*, 372, 666–669, 1994.
- Norman, J. M., Garcia, R., and Verma, S. B.: Soil surface CO₂ fluxes and the carbon budget of grasslands, *J. Geophys. Res.*, 97, 18845–18853, 1992.
- Oelbermann, M., Voroney, R. P., Thevathasan, N. V., Gordon, A. M., Kass, D. C. L., and Schlonvoigt, A. M.: Soil carbon dynamics and residue stabilization in a Costa Rican and southern Canadian alley cropping system, *Agroforest. Syst.*, 68, 27–36, doi:10.1007/s10457-005-5963-7, 2006.
- Ohashi, M., Kumagai, T., Kume, T., Gyokusen, K., Saitoh, T. M., and Suzuki, M.: Characteristics of soil CO₂ efflux variability in an aseasonal tropical rainforest in Borneo Island, *Biogeochemistry*, 90, 275–289, 2008.
- Parkinson, K. J.: An improved method for measuring soil respiration in the field, *J. Appl. Ecol.*, 18, 221–228, 1981.
- Quinn, W. H., Zopf, D. O., Short, K. S., and Yang, R.: Historical Trends and Statistics of Southern Oscillation, El Niño, and Indonesian Droughts, *Fish. Bull.*, 76, 663–678, 1978.
- R Development Core Team R: A language and environment for statistical computing. R Foundation for Statistical Computing: Vienna, Austria, ISBN 3-900051-07-0, online available at: <http://www.R-project.org>, 2008.
- Schwendenmann, L., Veldkamp, E., Brenes, T., O'Brien, J. J., and Mackensen, J.: Spatial and temporal variation in soil CO₂ efflux in an old-growth neotropical rain forest, La Selva, Costa Rica, *Biogeochemistry*, 64, 111–128, 2003.
- Schwendenmann, L. and Veldkamp, E.: Long-term CO₂ production from deeply weathered soils of a tropical rain forest: evidence for a potential feedback to climate warming, *Glob. Change Biol.*, 12, 1–16, 2006.
- Schwendenmann, L., Veldkamp, E., Moser, G., Hölscher, D., Köhler, M., Clough, Y., Anas, I., Djajakirana, G., Erasmi, S., Hertel, D., Leitner, D., Leuschner, C., Michalzik, B., Propastin, P., Tjoa, A., Tschardtke, T., and van Straaten, O.: Effects of an experimental drought on the functioning of a cacao agroforestry system, Sulawesi, Indonesia, *Glob. Change Biol.*, doi:10.1111/j.1365-2486.2009.02034.x, in press, 2010.
- Sheffield, J. and Wood, E. F.: Projected changes in drought occurrence under future global warming from multi-model, multi-scenario, IPCC AR4 simulations, *Clim. Dynam.*, 31, 79–105, 2008.
- Šimůnek, J., Šejna, M., Saito, H., Sakai, M., and van Genuchten, M. T.: *The Hydrus-1D Software Package for Simulating the One-Dimensional Movement of Water, Heat, and Multiple Solutes in Variably-Saturated Media*. Riverside, California, USA, 2008.
- Sivakumar, M. V. K., Das, H. P., and Brunini, O.: Impacts of present and future climate variability and change on agriculture and forestry in the arid and semi-arid tropics, *Clim. Change*, 70, 31–72, 2005.
- Sotta, E. D., Veldkamp, E., Guimaraes, B. R., Paixao, R. K., Ruivo, M. L. P., and Almeida, S. S.: Landscape and climatic controls on spatial and temporal variation in soil CO₂ efflux in an Eastern Amazonian Rainforest, Caxiuana, Brazil, *Forest Ecol. Manage.*, 237, 57–64, doi:10.1016/j.foreco.2006.09.027, 2006.
- Sotta, E. D., Veldkamp, E., Schwendenmann, L., Rocha Guimarães, B., Keila Paixão, R., de Lourdes P. Ruivo, M., Carlos Lola da Costa, A., and Meir, P.: Effects of an induced drought on the soil CO₂ production and soil CO₂ efflux in an Eastern Amazonian Rainforest, Brazil, *Glob. Change Biol.*, 13, 2218–2229, 2007.
- Tian, H., Melillo, J. M., Kicklighter, D. W., McGuire, A. D., Helfrich, J., Moore, B., and Vorosmarty, C. J.: Climatic and biotic controls on annual carbon storage in Amazonian ecosystems, *Glob. Ecol. Biogeogr.*, 9, 315–335, 2000.

- Timmermann, A., Oberhuber, J., Bacher, A., Esch, M., Latif, M., and Roeckner, E.: Increased El Nino frequency in a climate model forced by future greenhouse warming, *Nature*, 398, 694–697, 1999.
- Trumbore, S. and Druffel, E.: Carbon isotopes for characterizing sources and turnover of nonliving organic matter, in: *The Role of Nonliving Organic Matter in the Earth's Carbon Cycle*, edited by: Zepp, R. G. and Sontag, C. K., John Wiley and Sons, Chichester, 342, 1995.
- Veldkamp, E. and O'Brien, J. J.: Calibration of a Frequency Domain Reflectometry Sensor for Humid Tropical Soils of Volcanic Origin, *Soil Sci. Soc. Am. J.*, 64, 1549–1553, 2000.
- Wofsy, S. C., Harriss, R. C., and Kaplan, W. A.: Carbon-Dioxide in the Atmosphere over the Amazon Basin, *J. Geophys. Res.-Atmos.*, 93, 1377–1387, 1988.